The crossover between organized and disorganized states in some non-equilibrium systems

2009 J. Phys. A: Math. Theor. 42 195001

(http://iopscience.iop.org/1751-8121/42/19/195001)

IOP PUBLISHING JOURNAL OF PHYSICS A: MATHEMATICAL AND THEORETICAL

J. Phys. A: Math. Theor. **42** (2009) 195001 (20pp) doi:10.1088/1751-8113/42/19/195001

The crossover between organized and disorganized states in some non-equilibrium systems

Diego Luis González and Gabriel Téllez

Departamento de Física, Universidad de Los Andes A A 4976 Bogotá, Colombia

E-mail: die-gon1@uniandes.edu.co and gtellez@uniandes.edu.co

Received 7 November 2008, in final form 20 March 2009
Published 21 April 2009
Online at stacks.iop.org/JPhysA/42/195001

Abstract

We study numerically the crossover between organized and disorganized states of three non-equilibrium systems: the Poisson/coalesce random walk (PCRW), a one-dimensional spin system and a quasi one-dimensional lattice gas. In all cases, we describe this crossover in terms of the average spacing between particles/domain borders $\langle S(t)\rangle$ and the spacing distribution functions $p^{(n)}(s)$. The nature of the crossover is not the same for all systems; however, we found that for all systems the nearest neighbor distribution $p^{(0)}(s)$ is well fitted by the Berry–Robnik model. The destruction of the level repulsion in the crossover between organized and disorganized states is present in all systems. Additionally, we found that the correlations between domains in the gas and spin systems are not strong and can be neglected in a first approximation, but for the PCRW the correlations between particles must be taken into account. To find $p^{(n)}(s)$ with $n > 1$, we propose two different analytical models based on the Berry–Robnik model. Our models give us a good approximation for the statistical behavior of these systems at their crossover and allow us to quantify the degree of order/disorder of the system.

PACS numbers: 05.40.Fb, 05.50.+q, 45.70.Vn

(Some figures in this article are in colour only in the electronic version)

1. Introduction

Many one-dimensional non-equilibrium systems exhibit a crossover between disorganized and organized states. This crossover usually depends on the value of one or more parameters which set the system in one of these states. Our main objective is to study the statistical behavior of three non-equilibrium systems at their crossovers between organized and disorganized states. The first system is the Poisson/coalesce random walk (PCRW) where the particles describe independent random walks and when two particles meet they coalesce with probability k,

otherwise they interchange their positions. The second system is a quasi one-dimensional gas, where the particles interact only by volume exclusion in the presence of an external field. The last system is a one-dimensional spin lattice, where the particles interact by a coupling force J in the presence of an external driving field.

We propose two analytical models for the spacing distribution functions of these systems and compare them with the numerical results from the simulation. Our analytical models are based on the Berry–Robnik model introduced in [1]. This model is used in quantum systems which are neither integrable nor fully chaotic in order to find an analytical approximation to the nearest neighbor distribution of the energy levels of the system, see [1–3]. The Berry–Robnik model depends on one parameter which controls the crossover. The crossover is described through the nearest neighbor distribution $p^{(0)}(s)$, which gives us the probability that the distance between two consecutive levels is s. We complement the model proposed in [1] calculating analytically the higher order spacing distribution functions $p^{(n)}(s)$ for $n > 0$ and the pair correlation function $g(r)$ by two methods.

This paper is organized as follows. Because of its importance, in section 2 we explain in detail the Berry–Robnik model. In sections 3–5, we test our analytical models with three non-equilibrium systems: the Poisson/coalesce random walk, the quasi one-dimensional gas and the one-dimensional spin lattice, respectively. These systems are also explained in those sections.

2. The Berry–Robnik model as a non-equilibrium system

We consider a continuous one-dimensional ring with two kinds of particles A and B and normalized densities ρ_A and ρ_B, respectively. The particles A are subject to the reaction $A + A \to A$, i.e., they are coalescing random walkers. Particles B describe independent random walks and they are subject to the reaction $B \to 0$. The amount of particles B that disappear is calculated in such a way that the number of particles A, N_A, and the number of particles B, N_B, satisfy the relation $N_B/N_A =$ constant at each time step. This is the only interaction between both species of particles.

For this system, $P^{(n)}(S, t)$ is the probability that the distance between two particles is S at time t under the condition that between these particles there are n additional particles. When the average distance between neighbor particles is much smaller than the size of the lattice, the system exhibits a dynamical scaling for all values of ρ_A and ρ_B. In this regime, the spacing distributions can be scaled by using the variable change $s = S(t)/\langle S(t)\rangle$. Then, we obtain the time-independent spacing distributions $p^{(n)}(s)$.

It is known that in the scaling regime $N_A = L/(2\pi Dt)^{1/2}$ where D is the diffusion constant and L is the size of the lattice, see [4] for more information about the coalescing random walk (CRW). It is straightforward to show that $N_B = N_A\rho_B/(1-\rho_B)$, then the average length between nearest neighbors satisfies $\langle S(t)\rangle = (1 - \rho_B)(2\pi Dt)^{1/2}$.

The interaction between species warrants that the quotient between normalized densities ρ_A and ρ_B is always constant, i.e., the rate of disappearance of particles B is proportional to the rate of disappearance of particles A and the proportionality constant is ρ_B/ρ_A. Taking this into account, in the scaling regime, the system is the uncorrelated superposition of two independent systems of particles A and B with constant normalized densities. Our objective is to calculate the nearest neighbor distribution $p^{(0)}(s)$ of the whole system. This can easily be done because we have the superposition of two uncorrelated distribution functions $p_i^{(0)}(s)$ which satisfies

$$\langle s_i\rangle = \int_0^\infty \mathrm{d}s\, s p_i^{(0)}(s) = \frac{1}{\rho_i} \tag{1}$$

and

$$\int_0^\infty \mathrm{d}s\; p_i^{(0)}(s) = 1, \tag{2}$$

where $i = A$ or B and ρ_i is the density of particles corresponding to the system A or B. As is natural, the normalized densities satisfy $\rho_A + \rho_B = 1$.

Let $E^{(1)}(s)$ be the probability to choose randomly an empty segment of length s. This probability is related to $p^{(0)}(s)$. In order to prove this, we consider the probability that there are no particles in the interval q to $q + r$, given that there is a particle at q. This probability is given by $\int_r^\infty p^{(0)}(x)\,\mathrm{d}x$.

In our case, we have the uncorrelated superposition of two kinds of particles, then we can write

$$\int_r^\infty p^{(0)}(x)\,\mathrm{d}x = \rho_A q_B(r) \int_r^\infty p_A^{(0)}(y)\,\mathrm{d}y + \rho_B q_A(r) \int_r^\infty p_B^{(0)}(y)\,\mathrm{d}y, \tag{3}$$

where, for example, ρ_A is the probability that the particle in position q belongs to the system A, $\int_r^\infty p_A^{(0)}(x)\,\mathrm{d}x$ and $q_B(r)$ are the probabilities that there are no particles of the systems A and B in the interval, respectively. In order to find $q_B(r)$, we choose a particle randomly, the probability that the chosen point q lies within a gap of length σ to $\sigma + \mathrm{d}\sigma$ is proportional to $\sigma p_B^{(0)}(\sigma)$. To normalize this equation we use the fact that $\langle s_B \rangle = 1/\rho_B$, obtaining the probability distribution $\rho_B\,\mathrm{d}\sigma\,\sigma p_B^{(0)}(\sigma)$. Now, the probability that the distance to the next particle is r, given that the point is in the gap of length σ, is zero if $\sigma < r$ and $1/\sigma$ if $1 \leqslant r \leqslant \sigma$. The probability of not having a particle of the system B in an interval of length r is $(1 - r/\sigma)\theta(\sigma - r)$ (θ is the unit step function).

Thus, the unconditional probability that the distance until the next particle is r is given by

$$q_B(r) = \rho_B \int_r^\infty p_B^{(0)}(\sigma)(\sigma - r)\,\mathrm{d}\sigma. \tag{4}$$

The same argument can be made for the second term of equation (3). Thus equation (3) takes the form

$$\begin{aligned}\int_r^\infty p^{(0)}(x)\,\mathrm{d}x = {} & \rho_A \int_r^\infty p_A^{(0)}(y)\,\mathrm{d}y\; \rho_B \int_r^\infty p_B^{(0)}(\sigma)(\sigma - r)\,\mathrm{d}\sigma \\ & + \rho_B \int_r^\infty p_B^{(0)}(y)\,\mathrm{d}y\; \rho_A \int_r^\infty p_A^{(0)}(\sigma)(\sigma - r)\,\mathrm{d}\sigma.\end{aligned} \tag{5}$$

The probability $E^{(1)}(s)$ is the probability that $r > s$, then integrating equation (5) over r we find

$$E^{(1)}(s) = \int_s^\infty \mathrm{d}r \int_r^\infty \mathrm{d}x\; p^{(0)}(x) = \rho_A E_A^{(1)}(s) \rho_B E_B^{(1)}(s), \tag{6}$$

where we define

$$E_i^{(1)}(s) = \int_s^\infty \mathrm{d}\sigma\; p_i^{(0)}(\sigma)(\sigma - s) = \int_s^\infty \mathrm{d}\sigma \int_\sigma^\infty \mathrm{d}x\; p_i^{(0)}(x). \tag{7}$$

From equation (6), the spacing distribution function $p^{(0)}(s)$, which is the result of the mix of systems A and B, is given by

$$p^{(0)}(s) = \frac{\mathrm{d}^2 E^{(1)}(s)}{\mathrm{d}s^2}. \tag{8}$$

The fact that $E^{(1)}(s)$ is given by the product of $E_i^{(1)}(s)$ functions is natural, because we used two statistical independent sequences. It is easy to prove that the $E_i^{(1)}(s)$ functions satisfy

$$E_i^{(1)}(0) = \frac{1}{\rho_i} \tag{9}$$

and

$$\frac{\mathrm{d}E_i^{(1)}(0)}{\mathrm{d}s} = -1. \tag{10}$$

From the above equations it follows that $p^{(0)}(0)$ is given by

$$p^{(0)}(0) = 1 + \rho_A\big(p_A^{(0)}(0) - \rho_A\big) + \rho_B\big(p_B^{(0)}(0) - \rho_B\big). \tag{11}$$

Then, even if $p_A^{(0)}(0) = 0$ and $p_B^{(0)}(0) = 0$ it can happen that $p^{(0)}(0) \neq 0$. In our particular case, we superpose one Wigner distribution

$$p^{(0)}(s, \rho_A) = \frac{\pi}{2}\rho_A^2 s \exp\left[-\frac{\pi}{4}\rho_A^2 s^2\right] \tag{12}$$

with density ρ_A and one Poisson distribution

$$p^{(0)}(s, \rho_B) = \rho_B \exp[-\rho_B s] \tag{13}$$

with density ρ_B, then we have

$$p^{(0)}(s, q) = \mathrm{e}^{-qs}\left(q^2\mathrm{erfc}\left(\frac{\sqrt{\pi}}{2}(1-q)s\right) + \left(2q(1-q) + \frac{\pi}{2}(1-q)^3 s\right)\mathrm{e}^{-\frac{\pi}{4}(1-q)^2 s^2}\right), \tag{14}$$

where $\rho_B \equiv q$ is the density of the Poisson sequence, $\rho_A = 1 - q$ is the one for the Wigner sequence and $\mathrm{erfc}(z)$ is the complementary Gaussian error function. Note that equation (14) reduces to the Poisson distribution for $q = 1$, and for $q = 0$ it reduces to the Wigner distribution. This result is well known in random matrix theory and corresponds to the Berry–Robnik model for the crossover between chaotic and non-chaotic behavior in quantum systems; see [1].

2.1. Higher spacing distribution functions

In [5, 6] the authors show that the nearest neighbor distribution is not enough to describe the complete statistical behavior of a non-equilibrium system, because several different systems could share the same nearest neighbor distribution. Because of this, we generalize the Berry–Robnik model for higher spacing distribution functions. Let $E^{(n)}(x_1, y_1, \ldots, x_n, y_n)$ be the joint probability that the intervals $[x_i, y_i]$ $(i = 1, 2, \ldots, n)$ are empty. The intervals are non-overlapping and ordered, $x_1 < y_1 < \cdots < x_n < y_n$. Because of the independent superposition nature of the Berry–Robnik model, $E^{(n)}(x_1, y_1, \ldots, x_n, y_n)$ can be written as

$$E^{(n)}(x_1, y_1, \ldots, x_n, y_n) = \rho_A^n E_A^{(n)}(x_1, y_1, \ldots, x_n, y_n)\rho_B^n E_B^{(n)}(x_1, y_1, \ldots, x_n, y_n), \tag{15}$$

where $E_A^{(n)}(x_1, y_1, \ldots, x_n, y_n)$ and $E_B^{(n)}(x_1, y_1, \ldots, x_n, y_n)$ are the joint probabilities for particles A and B, respectively. The authors of [7] showed that spacing distribution functions $p^{(n)}(s)$ can be calculated from equation (15); let us summarize their most important result. Let $p^{(n)}(s)$ be the probability that given one particle its $(n+1)$th neighbor is at a distance s. From its definition $p^{(n)}(s)$ is given by

$$p^{(n)}(s) = \int_{0<y_1<\cdots<y_n<s} \omega^{(n+2)}(0, y_1, \ldots, y_n, s)\,\mathrm{d}y_1 \cdots \mathrm{d}y_n, \tag{16}$$

with

$$\omega^{(n)}(x_1, \ldots, x_n) = -\left.\frac{\partial^n E^{(n-1)}(x_1, y_1, \ldots, x_{n-1}, y_{n-1})}{\partial x_1 \cdots \partial x_{n-1}\partial y_{n-1}}\right|_{y_1=x_2,\ldots,y_{n-1}=x_n}. \tag{17}$$

On the other hand, it is well known that for the CRW, $E_A^{(n)}(x_1, y_1, \ldots, x_n, y_n)$ is given by [4]

$$E_A^{(n)}(x_1, y_1, \ldots, x_n, y_n) = \sum_p \sigma_p E_A^{(1)}(z_{1,p}, z_{2,p}) \cdots E_A^{(1)}(z_{2n-1,p}, z_{2n,p}), \tag{18}$$

where $z_{1,p}, z_{2,p}, \ldots, z_{2n,p}$ symbolizes an ordered permutation, p, of the variables $x_1, y_1, \ldots, x_n, y_n$, such that

$$z_{1,p} < z_{2,p}, z_{3,p} < z_{4,p}, \ldots, z_{2n-1,p} < z_{2n,p}, \tag{19}$$

$$z_{1,p} < z_{3,p} < z_{5,p} < \cdots < z_{2n-1,p}. \tag{20}$$

In equation (18), σ_p is the signature of the permutation, i.e., $\sigma_p = 1$ for even permutations and $\sigma_p = -1$ for odd permutations.

The function $E_A^{(1)}(x_1, y_1)$ is the probability that from x_1 to y_1 the lattice is empty. Then it is possible to generate the complete solution for the CRW from $E_A^{(1)}(x_1, y_1)$, which is given by the solution of the diffusion equation under the suitable boundary conditions (see [4]). In fact, the exact expression for this function is

$$E_A^{(1)}(x_1, y_1) = \frac{1}{\rho_A}\operatorname{erfc}\left(\frac{\sqrt{\pi}\rho_A}{2}(y_1 - x_1)\right), \tag{21}$$

for additional information see [4, 8]. The particles B describe independent random walks, then we have

$$E_B^{(1)}(x_1, y_1) = \frac{1}{\rho_B}\,\mathrm{e}^{-\rho_B(y_1 - x_1)} \tag{22}$$

and

$$E_B^{(n)}(x_1, y_1, \ldots, x_n, y_n) = \prod_{i=1}^{n} \frac{1}{\rho_B^n}\,\mathrm{e}^{-\rho_B(y_i - x_i)}. \tag{23}$$

From equations (15), (18), (21) and (23) we can calculate $E^{(n)}(x_1, y_1, \ldots, x_n, y_n)$ for the whole system and then we can use (16) and (17) to calculate $p^{(n)}(s)$. By using this formalism it is also possible to calculate the n-point correlation function

$$\rho^{(n)}(x_1, \ldots, x_n) = (-1)^n \frac{\partial^n}{\partial y_1 \cdots \partial y_n} E^{(n)}(x_1, y_1, \ldots, x_n, y_n)|_{y_1 = x_1, \ldots, y_n = x_n}, \tag{24}$$

in fact, the pair correlation function is given by

$$g(r) = 1 - (1-q)^2\,\mathrm{e}^{-\frac{\pi}{2}(1-q)^2 r^2} + \frac{\pi}{2}\,\mathrm{e}^{-\frac{\pi}{4}(1-q)^2 r^2}(1-q)^3 r \operatorname{erfc}\left(\frac{\sqrt{\pi}}{2}(1-q)r\right). \tag{25}$$

The above equation takes the form $g(r) = 1$ for $q = 1$. For $q = 0$ we recover the pair correlation function of the CRW; see [4].

3. A simple model of the crossover between organized and disorganized states: the Poisson/coalesce random walk

Consider a one-dimensional ring with L sites and n_p particles, then the particle density is given by $\rho = n_p/L$. The particles describe independent random walks and when two particles meet they coalesce with probability k, otherwise they interchange their positions. This system was studied previously in [9, 10]. The algorithm used in the simulation is as follows:

(1) n_p particles are randomly inserted in an L site lattice.
(2) A particle is chosen at random.
(3) The particle can move to the left or to the right with the same probability. If the particle is moved to an occupied site, the particles coalesce with probability k or they interchange their positions with probability $1 - k$.
(4) In a time unit all particles are moved.

In the limit $t \gg 1$, finite systems reach a non-equilibrium steady state (NESS), where there is only one particle which executes a simple random walk and $\langle S(t)\rangle = L$. As we will see soon, for an infinite-size system in the same limit, the average length between nearest neighbor particles grows as $t^{1/2}$ for $k > 0$ and the system is statistically equivalent to the CRW.

It is possible to derive an approximate analytical solution by using the inter-particle distribution function method (IPDF), see [4, 9]. Let E_n be the probability to find an empty segment of length n in the lattice. The master equation for E_n can be written as

$$\frac{\partial E_n(t)}{\partial t} = \frac{2D}{\Delta x^2}(E_{n+1}(t) - 2E_n(t) + E_{n-1}(t)) + \frac{2D}{\Delta x^2}(k-1)P(\overbrace{\circ\cdots\circ}^{n-1}\bullet\bullet), \tag{26}$$

with boundary conditions $E_0(t) = 1$ and $E_\infty(t) = 0$. The probability $P(\overbrace{\circ\cdots\circ}^{n-1}\bullet\bullet)$ cannot be written in terms of $E_n(t)$. However in [4, 9] the authors propose an approximation for this probability

$$P(\overbrace{\circ\cdots\circ}^{n-1}\bullet\bullet) \approx \frac{P(\overbrace{\circ\cdots\circ}^{n-1}\bullet)P(\bullet\bullet)}{P(\bullet)}, \tag{27}$$

which can be written in terms of $E_n(t)$ as

$$P(\overbrace{\circ\cdots\circ}^{n-1}\bullet\bullet) \approx \frac{(1-2E_1+E_2)(E_{n-1}-E_n)}{1-E_1}. \tag{28}$$

This approximation allows us to calculate the concentration of particles $c(t) = 1/\langle S(t)\rangle$. From equations (26) and (28) and summing over the index n it is easy to find

$$\sum_{n=1}^{\infty}\frac{\partial E_n(t)}{\partial t} = \frac{2D}{\Delta x^2}(E_0(t) - E_1(t)) - \frac{2D}{\Delta x^2}(1-k)\frac{(1-2E_1(t)+E_2(t))}{1-E_1(t)}E_0(t). \tag{29}$$

Taking into account that $\partial_t E_1(t) = 2Dk(1-2E_1+E_2)/\Delta x^2$ and making the approximation $\sum_{n=1}^{\infty} E_n(t) \approx (2/\pi)/(1-E_1(t))$, in [9] it is found that

$$\frac{2}{\pi}\frac{\mathrm{d}}{\mathrm{d}\tau}\left(\frac{1}{c(\tau)}\right) = c(\tau) + \frac{(1-k)}{kc(\tau)}\frac{\mathrm{d}c(\tau)}{\mathrm{d}\tau}, \tag{30}$$

where $\tau = 2Dt/\Delta x^2$ and $c(\tau) = 1 - E_1(\tau)$. Equation (30) can be integrated obtaining

$$c(\tau) = \frac{2c_0^2 k}{c_0^2(k-1)\pi + \sqrt{c_0^2(-2k + c_0(k-1)\pi)^2 + 4c_0^4k^2\pi\tau}}, \tag{31}$$

with $c_0 \equiv c(0)$. Note that for $\tau \to \infty$, we have $c(\tau) \propto \tau^{-1/2}$ as we mentioned above. In figure 1, we show the behavior of $\langle S(t)\rangle = 1/c(\tau)$ for different values of k, this result was first shown in [9]. The agreement between equation (31) and the simulation is very good. Because of the finite-size effects in the simulation, for $L = 500$, the system does not reach $\beta = 1/2$, $\langle S(t)\rangle \propto t^\beta$, but for $L = 10000$ we can see this regime for $k = 1, k = 0.25, k = 0.02$ and $k = 0.01$. For low values of k, the time during which the system remains disorganized with $\langle S(t)\rangle$ almost constant is larger than for large values of k.

The nearest neighbor distribution $p^{(0)}(s)$ evolves in the following way. The system starts in a disorganized state in such a way that $p^{(0)}(s)$ is described by the Poisson distribution, then for $k \neq 0$ the system evolves and $p^{(0)}(s)$ is deformed continuously until it reaches the Wigner distribution, for large systems. For small systems, the finite-size effects appear before this

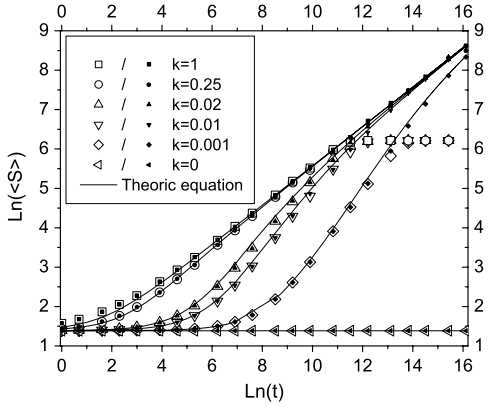

Figure 1. Behavior of $\langle S\rangle$ as a function of t. In the simulation, we took two lattices with $L = 10000$ (filled symbols) and $L = 500$ (empty symbols) over 500 realizations. In both cases, the initial density was $1/4$. The continuous line represents equation (31).

regime is attained, i.e., small systems reach the NESS without reaching the scaling regime. In the $k = 0$ case, the system remains disorganized for all values of t.

In the continuum limit, equation (26) takes the form

$$\frac{\partial E^{(1)}(x,t)}{\partial t} = 2D\frac{\partial^2 E^{(1)}(x,t)}{\partial x^2} + 2D(k-1)\frac{\partial E^{(1)}(x,t)}{\partial x}\frac{\frac{\partial^2 E^{(1)}(x,t)}{\partial x^2}\Big|_{x=0}}{\frac{\partial E^{(1)}(x,t)}{\partial x}\Big|_{x=0}}, \qquad (32)$$

with boundary conditions $E^{(1)}(0,t) = 1$ and $E^{(1)}(\infty,t) = 0$. This equation can easily be solved for $k = 1$. For arbitrary values of k, equation (32) cannot be solved exactly; however, some approximate expressions were found in [4, 9, 10], but they involve self-consistent forms which are difficult to handle. Motivated by this fact, we propose to use the Berry–Robnik model to find an approximate analytical solution to the statistical behavior of this system.

Equation (14) provides a good fit for the crossover in this reaction–diffusion model during its time evolution as we can see in figure 2. For the nearest neighbor distribution, the fit is almost perfect for low and high values of s, but for intermediate values we can see little differences in the interval $0.25 < s < 1$ for intermediate values of k. In this figure, all data were taken at different times with $k = 0.05$ over 20000 realizations, the initial density was 0.1. The fit parameter is q. We found the appropriate value of q by using the numerical results for $p^{(0)}(s)$, equation (14) and the minimum square criteria[1].

The higher spacing distributions have been calculated with two methods. In the first one, we use our extension for the original Berry–Robnik equation (15) with equation (16). From now on, we call it the generalized Berry–Robnik (GBR) model. For the second one, we use equation (14) with the independent interval approximation (IIA). We call this method the Berry–Robnik+IIA (BR+IIA) model. In the IIA approximation, the entire statistical behavior of the system is described by the nearest neighbor distribution $p^{(0)}(s)$ and the joint probability

[1] This can also be done for values of k near to 1 or long times by using the numerical value of $p^{(0)}(0)$ obtained from the simulation and taking into account that $p^{(0)}(0) = 2q - q^2$ for the Berry–Robnik model.

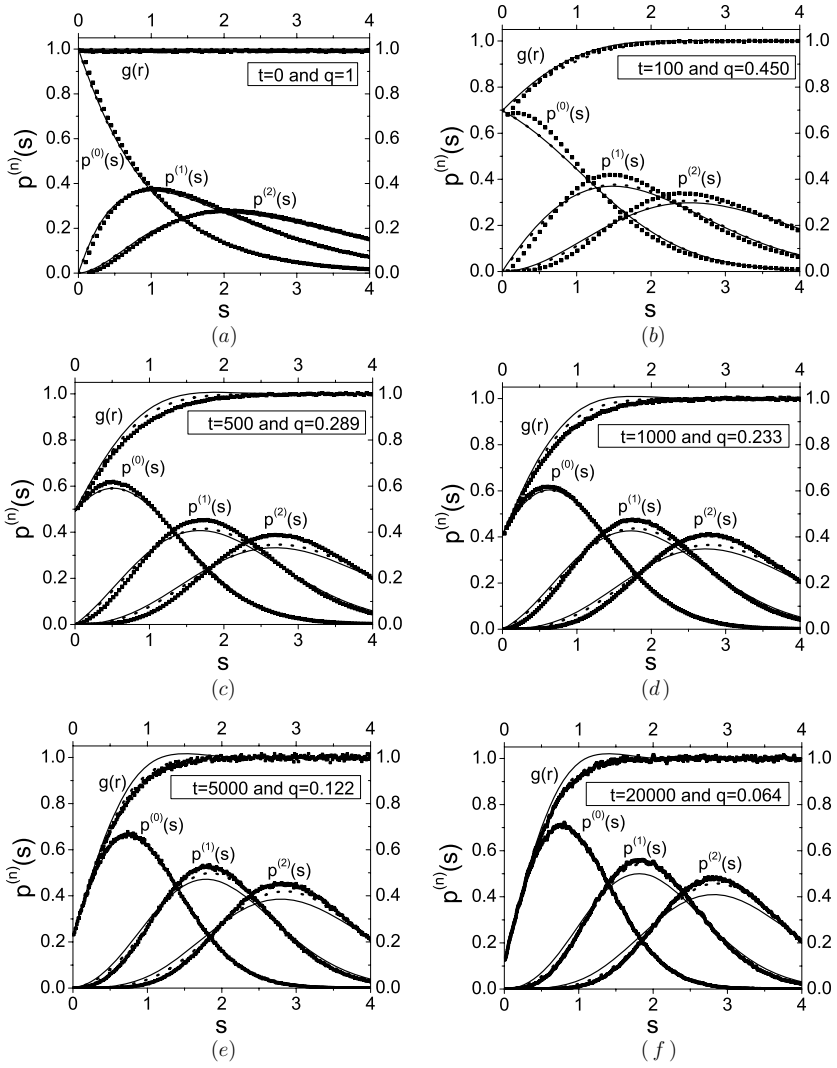

Figure 2. Crossover between the Poisson and the Wigner distribution for the PCRW, for $k = 0.05$, for various times t. The continuous line corresponds to the BR+IIA model, the dashed line corresponds to the GBR model and the square dots correspond to the simulation.

to find the particles in positions $x_1, \ldots, x_N$ can be written as the product of independent products of the N nearest neighbor distributions,

$$P_N(x_1, \ldots, x_N) = \frac{1}{Z_N} p^{(0)}(x_2 - x_1) \cdots p^{(0)}(x_N - x_{N-1}) p^{(0)}(x_1 + L - x_N), \tag{33}$$

where the partition function Z_N is the normalization constant

$$Z_N = \int_{x_1 < x_2 < \cdots < x_N < x_1 + L} \mathrm{d}x_1, \ldots, \mathrm{d}x_N \prod_{i=1}^{N} p^{(0)}(x_{i+1} - x_i). \tag{34}$$

In the IIA approximation, the correlations among intervals $[x_1, x_2], \ldots, [x_{N-1}, x_N]$ are neglected; for a review of this method see [5]. As is natural, the generalized Berry–Robnik

model and the Berry–Robnik+IIA model are equivalent in the limit $q \to 1$ because in this regime those correlations are not strong and can be neglected.

In general, for the PCRW the fits are better for the GBR model than the BR+IIA. This means that for this system the information contained in $p^{(0)}(s)$ is not enough to describe the entire statistical behavior of the system, i.e., the correlation among intervals cannot be neglected as is done in the BR+IIA model. These correlations can be neglected only for small times ($\tau \leqslant \tau_1$), when the particles do not coalesce enough to build strong correlations between them. The value of τ_1 as a function of k can be computed from equation (30) as follows. Integrating equation (30), it is easy to find

$$\tau = \frac{1-k}{k}(\langle S(\tau)\rangle - \langle S(0)\rangle) + \frac{1}{\pi}(\langle S(\tau)\rangle^2 - \langle S(0)\rangle^2). \tag{35}$$

Because of the reaction between particles, $\langle S(\tau)\rangle$ grows in time for $k > 0$ making it possible to write $\langle S(\tau)\rangle$ as $\langle S(0)\rangle$ plus an increment $\langle \Delta S\rangle$. In this way, equation (35) takes the form

$$\tau = \frac{1-k}{k}\langle \Delta S\rangle + \frac{1}{\pi}\langle \Delta S\rangle^2 + \frac{2}{\pi}\langle \Delta S\rangle\langle S(0)\rangle. \tag{36}$$

The correlations between particles can be neglected for small times when $\langle \Delta S\rangle \ll 1$, then we can neglect $\langle \Delta S\rangle^2$ in equation (36). Finally if we consider that $\langle \Delta S\rangle$ must be a fraction ϵ of $\langle S(0)\rangle$, we find

$$\tau_1 = \epsilon\left(\frac{1-k}{k}\langle S(0)\rangle + \frac{2}{\pi}\langle S(0)\rangle^2\right). \tag{37}$$

This equation was derived first in [9]. From equation (37), it is clear that there is a time when the interaction between particles goes unnoticed even in the case of $k = 1$, where τ_1 is the typical time that one particle needs to reach one of its nearest neighbors. In the limit $k \to 0$, we have $\tau_1 \to \infty$ as is natural because in this case $\langle S(\tau)\rangle$ is a constant.

We conclude that for the PCRW the spacing distribution and the pair correlation functions can be approximated from the uncorrelated superposition of a Poisson and a Wigner distribution function as is proposed in the GBR model.

An alternate way to analyze the crossover of this system is to study the spacing distribution functions at a fixed given time, but for different values of k. In order to establish a connection between this picture for the transition and that shown in figure 2, it is necessary to find the correct combination of k and τ which gives the same statistical behavior for different values of these parameters. To find it, in figure 3(a) we show the behavior of q as a function of τ for different values of k. We found that making the change of variable

$$\tilde{\tau} = \tau k^2/(1-k)^2, \tag{38}$$

all lines shown in figure 3(a) collapse into a single one; see figure 3(b). Then, different combinations of k and τ with fixed $\tau k^2/(1-k)^2$ give the same statistical behavior, i.e., give the same value for the fit parameter q. This is shown in figure 4; the data were taken in all cases over 20000 realizations with $\tau k^2/(1-k)^2 \approx 13.9$. For large values of $\tilde{\tau}$, $\tilde{\tau} \gg 1$, we found that $q \propto \tilde{\tau}^{-0.5}$ and for low values of $\tilde{\tau}$, $\tilde{\tau} \ll 1$, $q \propto \tilde{\tau}^{-0.25}$.

The physical meaning of the change of variable (38) is clear if we introduce the crossover time, τ_2, between the intermediate regime (which starts when $\tau > \tau_1$) and the long-time regime (when k renormalizes to 1). This time is estimated in [9], by expanding equation (31) in powers of $1/\sqrt{\tau}$,

$$\tau_2 \propto \frac{(1-k)^2}{k^2}, \tag{39}$$

which is precisely the scaling factor used in figure 3(b). The change of variable (38) is $\tilde{\tau} = \tau/\tau_2$.

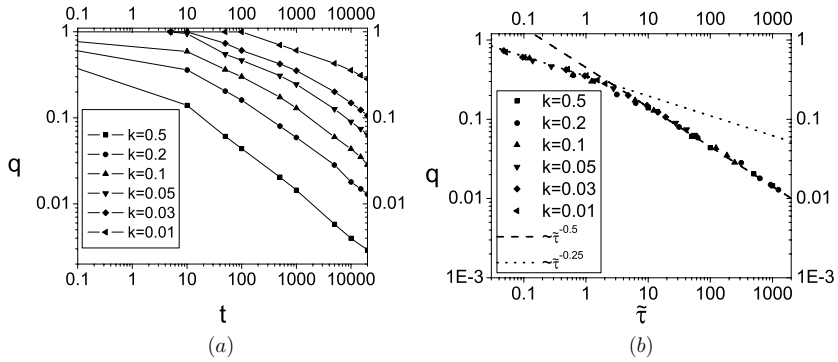

(*a*) (*b*)

Figure 3. Behavior of the fit parameter q as a function of t for different values of k.

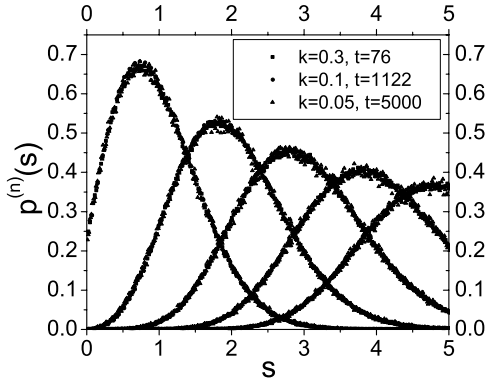

Figure 4. Statistical behavior for the PCRW for different values of k and t with $\tau k^2/(1-k)^2 \approx 13.9$, in all cases $q \approx 0.112$.

4. Crossover in the quasi one-dimensional gas system

This system was originally studied in [11]. There, the authors studied the biased diffusion of two species in a fully periodic $2 \times L$ rectangular lattice half filled with two types of particles labeled by their charge, there are $L/2$ particles with charge + and $L/2$ particles with charge $-$. An infinite external field drives the two species in opposite directions along the x-axis (the long axis). The only interaction between particles is an excluded volume constraint, i.e., each lattice site can be occupied by only one particle. The system evolves in time according to the following dynamical rules:

(1) L particles are randomly inserted in a $2 \times L$ rectangular lattice, $\frac{L}{2}$ particles (+) and $\frac{L}{2}$ particles $(-)$, the remaining sites are empty. Periodic boundary conditions are imposed in both directions of the lattice. Let the x-axis be the long axis of length L.

(2) Two neighbor sites are chosen at random. The contents of the sites are exchanged with probability 1 if the neighbor sites are particle–hole, but if they are particle–particle the contents are exchanged with probability γ. The exchanges which result in $+/-$ particles moving in the positive/negative x-direction are forbidden due to the action of the external field.

(3) A time unit corresponds to $2L$ attempts at exchange.

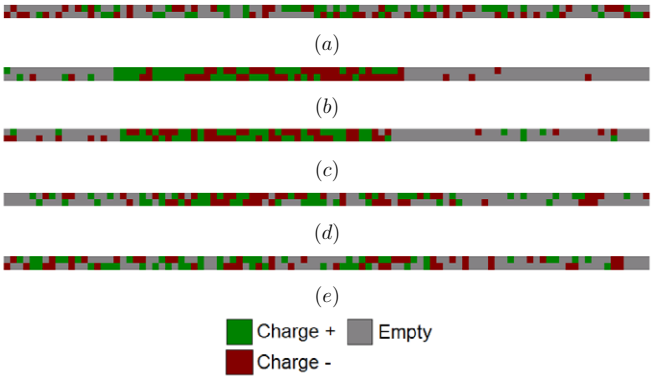

Figure 5. Typical configurations for the gas system in the NESS, for different values of γ from the same initial configuration. (a) Initial configuration, (b) $\gamma = 0.1$, (c) $\gamma = 0.3$, (d) $\gamma = 0.5$ and (e) $\gamma = 1$ for $t = 10000$.

With these dynamical rules, this system evolves with formation of domains for low values of γ; see figures 5(b) and (c). In this regime, the average length of domains grows in time and while the size of the domains remains much smaller than the total size L of the system, the domain-size distribution exhibits a dynamic scaling. In the long-time limit, the system reaches a non-equilibrium steady state (NESS) where there is only one macroscopic domain. The length of the macroscopic domain depends on γ, for example, for $\gamma = 0.1$. it has an approximate size of $L/2$. Additionally, for low values of γ, this macroscopic domain does not have a simple charge distribution and it almost contains no holes. The macroscopic domain is not in equilibrium because there are particles (travelers) which leak out from one end of this domain and travel along the lattice until they reach the other end of this domain; see figure 5(b). In the case of large values of γ the system remains homogeneous, i.e., disorganized without domain formation, as we can see in figure 5(e). For intermediate values of γ, the macroscopic domain is not well formed, it has many holes and it is unstable. In this case, there are many travelers and small length domains; see figure 5(d).

In order to obtain quantitative results, we measure the length of a domain by using the coarse-grained approximation (CG) defined in [11]. This approximation allows us to map the quasi one-dimensional lattice into a one-dimensional lattice. For any configuration on the $2 \times L$ lattice, we construct an effective one-dimensional one, with occupation numbers 0 or 1 on an L site line, as follows. At each site i, we assign 0 if there are five or less particles in the ten sites around it, including the ith column of the original lattice. We assign 1 otherwise, then we assign 1 in the ith site of the one-dimensional lattice if there are more particles than holes in the ten sites around the ith column in the original lattice[2]. In this simplified description, a domain is a simple consecutive sequence of ones and its size is just the length of this string.

In figure 6, we show the behavior of $\langle S(t) \rangle$ for six values of γ. The NESS behavior is evident in the long-time limit, when $\langle S(t) \rangle$ reaches its maximum value which depends on γ. Additionally, we found that in the NESS regime $\langle S(t) \rangle$ also depends on the size of the lattice

[2] In our description, we take only four neighbor lines around the ith column, two at the left and two at the right. This choice is arbitrary, however the results are not so sensitive to it. If we take less neighbor lines, we improve the measure of the small domains getting worse the measure of big domains and vice versa. Our choice of four neighbor lines gives us a reasonable measure of small and big domains.

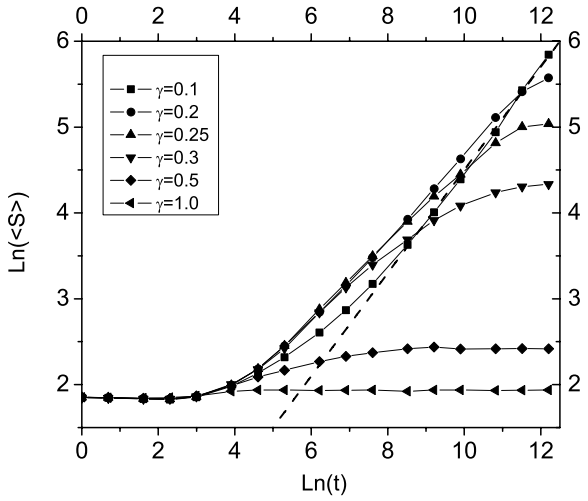

Figure 6. Behavior of $\langle S(t)\rangle$ for different values of γ, the dashed line is a reference line with slope 0.6. We used $L = 1000$.

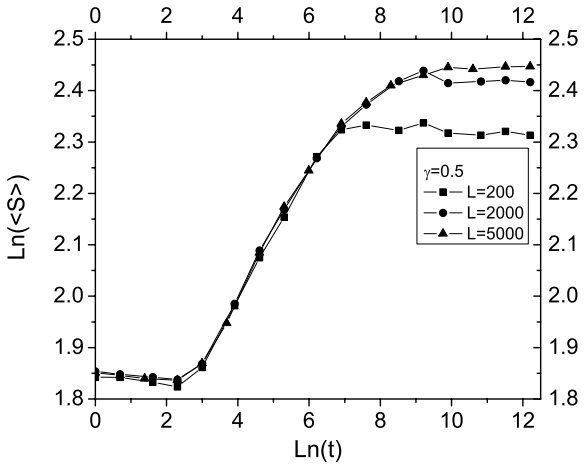

Figure 7. Average length of domains $\langle S(t)\rangle$ in the NESS regime for different values of L.

L for all values of γ, in fact for $\gamma = 0.1$ it is well known that $\langle S(t)\rangle \approx L/2$. In figure 7, we show $\langle S(t)\rangle$ for $\gamma = 0.5$ and different values of L. The value of $\langle S(t)\rangle$ increases with the value of L and we can expect that it reaches its maximum value in the limit $L \to \infty$. We can conclude that for finite systems $\langle S(t)\rangle$, in the NESS, depends on γ and L.

For $\gamma = 0.1$, we found in the scaling regime $\langle S(t)\rangle \propto t^{0.6}$, this result coincides with that found in [11]. For lower values of γ it seems that there is also a dynamical scaling region whose size decreases when γ increases. Naturally, for $\gamma = 1$ the systems remain homogeneous. Note that $\langle S(t)\rangle$ is very different for $\gamma = 0.1$ and $\gamma = 0.3$ cases, because for $\gamma = 0.3$ there are more travelers than in $\gamma = 0.1$; see figure 5.

In figure 8, we show the spacing distribution and the pair correlation functions for the gas system for different values of γ. As can be expected, the CG description is not appropriate to

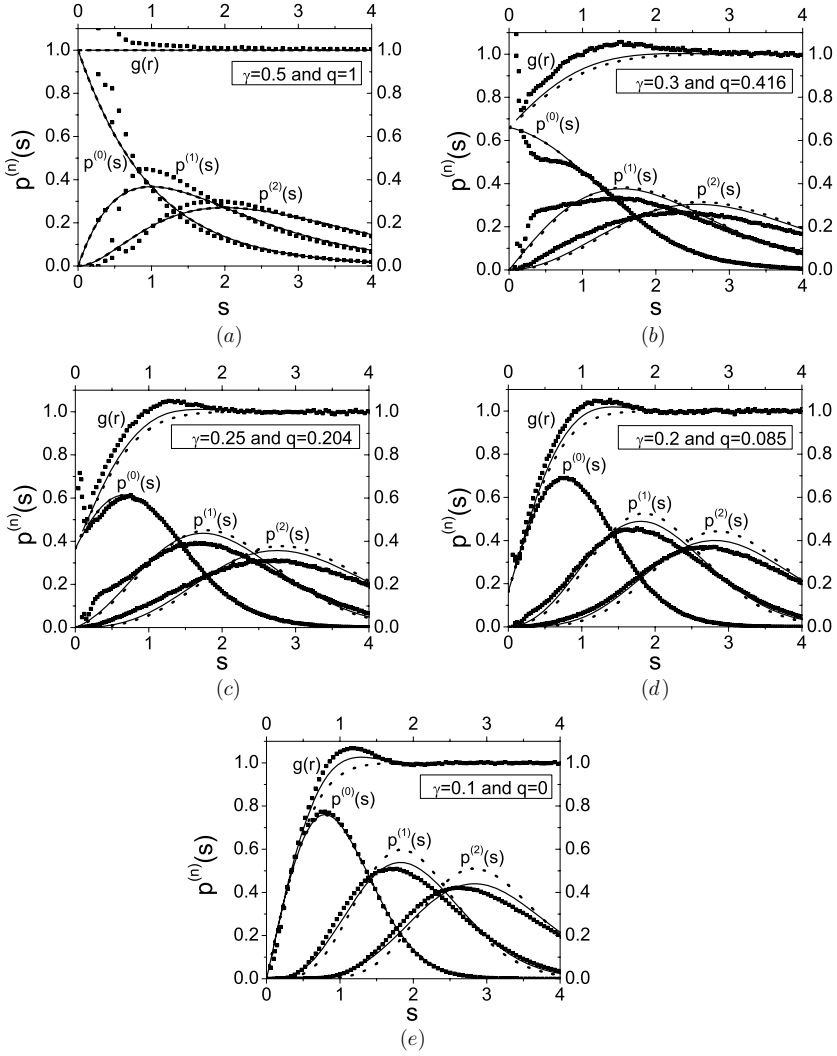

Figure 8. Crossover for the gas system. The continuous line corresponds to the BR+IIA model, the dashed line corresponds to the GBR model and the square dots correspond to the simulation.

measure the length of small domains. However, this method allows us to measure the length of big domains. For all values of γ, the nearest neighbor spacing distribution function is well fitted by the Berry–Robnik model for high values of s. For small values of γ, $p^{(0)}(s)$ is well described by the Wigner distribution. In the case of $\gamma = 1$, the nearest neighbor distribution is described by the Poisson distribution. However, the generalized Berry–Robnik model does not describe the next spacing distributions nor the pair correlation function with enough precision. The differences between the pure coalescing random walk (PCRW for $k = 1$) and the gas system were already studied in [5] for the case of $\gamma = 0.1$. There the authors found that the independent interval approximation (IIA) is a better model for the gas system than the CRW model. The results that we found for the Berry–Robnik+IIA model are shown in figure 8. We can see that the Berry–Robnik+IIA model is a better approximation for the statistical behavior

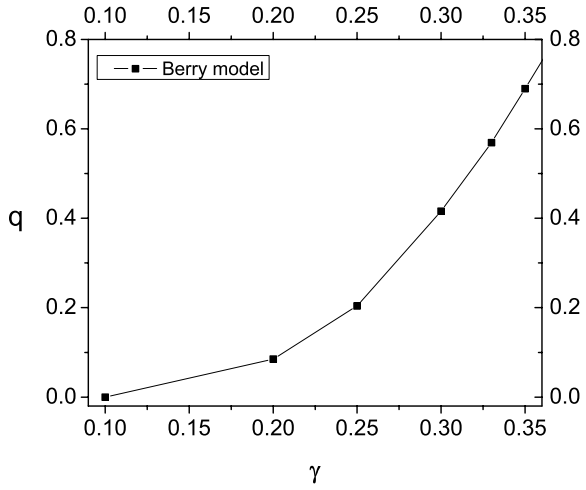

Figure 9. Behavior of q in the gas system for different values of γ.

of the gas for all values of γ. This fact suggests that, as it happens for $\gamma = 1$, the domains in this system are not strongly correlated for all values of γ and because of that those correlations can be neglected.

In figure 9, we show the behavior of q as a function of γ in the interval $[0.1, 0.35]$. We found that at least for $\gamma > 0.4$ the system is in a disorganized state, i.e., its statistical behavior is well described by the Poisson distribution for large values of s and fits give $q \approx 1$. In all fits used to find q as a function of γ we eliminated the regions where the points are highly dispersed, i.e., where the coarse-grain method does not measure the length of domains with enough precision.

The numerical results shown in figures 8 and 9 were obtained using a 2×1000 lattice over 20000 realizations, the data were taken at three different times $t = 2000$, $t = 3000$ and $t = 4000$. The results shown in figure 6 were obtained by using the same lattice over 500 realizations.

5. Crossover in the spin system

This system was originally introduced in [12]. There, the authors consider a lattice of length L with $L\mu$ spins up ('+') and $L(1-\mu)$ spins down ('−') with $0 < \mu < 1$. Periodic boundary conditions are imposed. The spin–flip events are as follows:

(1) $++--\leftrightarrow +-+- \quad \Delta = 4J - E.$
(2) $--++\leftrightarrow -+-+ \quad \Delta = 4J + E.$
(3) $++-+\leftrightarrow +-++ \quad \Delta = -E.$
(4) $-+--\leftrightarrow --+- \quad \Delta = -E.$

The transition probability rate for a process from left to right is $e^{-\frac{\Delta}{T}}$ for $\Delta > 0$ and 1 for $\Delta \leqslant 0$. The constant J is the nearest neighbor coupling between spins, E is the energy associated with an external field which drives the up ('+') spins to the right and the down ('−') spins to the left, and T is the thermal energy (temperature times Boltzmann constant).

In [12], the authors restrict their study to the regime $T \ll E \ll J$. In this regime, the microscopic dynamics of the lattice of spins may be mapped into one for an array domain

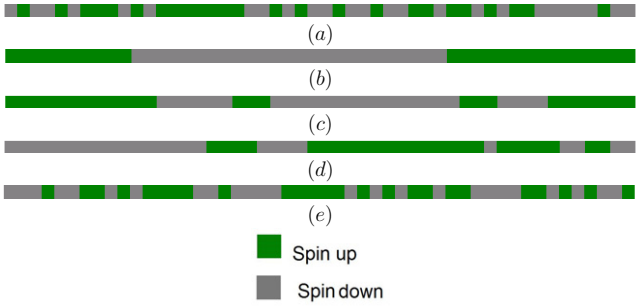

Figure 10. Typical configurations for the spin system in the NESS for different values of J from the same initial configuration. (a) Initial configuration, (b) $J = 2$, (c) $J = 1.5$, (d) $J = 1$ and (e) $J = 0.1$. We use $L = 50$, $\mu = 0.5$ and $t = 100000$.

dynamics, which provides a good approximation in this regime; for more information see [5, 6, 8, 12, 13]. With this macroscopic description in [5], the authors show that this system has statistical behavior very similar to that of the gas system. Additionally, the system exhibits dynamical scaling behavior and, in the long-time limit, the system reaches the NESS, where there are two macroscopic domains which move in opposite directions. However, this domain model does not allow us to study the crossover of the system between organized and disorganized states because it is valid only in the regime $T \ll E \ll J$. To study the crossover regime, we must use the microscopic dynamical rules listed above. In all simulations, we took $E = 1$ and $T = 1$.

In figure 10(b), we can see the asymptotic state for the spin system for large values of J where there are only two stable macroscopic domains and $\langle S(t)\rangle = L/2$. For $J = 0.1$, domain formation is not perceptible; see figure 10(e) which is almost identical to the disorganized initial state figure 10(a). However, as we will see soon, the average length of domains is different in both cases. In the NESS, for low values of J there is domain destruction and formation, in such a way that $\langle S(t)\rangle$ is constant with a value lower than $L/2$. As we can see in figure 11, for low values of J, the statistical behavior of the spin system in the NESS is well described by the Poisson distribution. This means that the system remains in a disorganized state where the average length of domains is bigger than the initial one ($\langle S(0)\rangle = 2$). We can see slight differences near $s = 0$, this happens because we used in our simulation a discrete finite lattice.

In figure 12, we can see the average length of domains $\langle S(t)\rangle$ as a function of time t. In this case, the behavior of $\langle S(t)\rangle$ is different from that found in the PCRW and in the gas system. For large values of J, the spin system reaches metastable states where $\langle S(t)\rangle$ is almost constant. Note that in all cases, the metastable state starts when the domain density is $1/4$, i.e., when the system, in the statistical average sense, is filled with domains of the form $++--++--$. This is a consequence of the microscopical dynamical rules that we use, because they take into account interaction among four neighboring spins. For large enough values of J, these domains have a low probability of destruction setting the system into a metastable state. In figure 13, we show the spacing distribution function in the metastable states, level repulsion is present. After some time, $\langle S(t)\rangle$ starts to grow again in time. In the PCRW and in the gas systems, the metastable states are not present. Once the metastable states end, the domain formation in the system continues in such a way that the average size of domains increases again. The length in time of these metastable states depends on the value

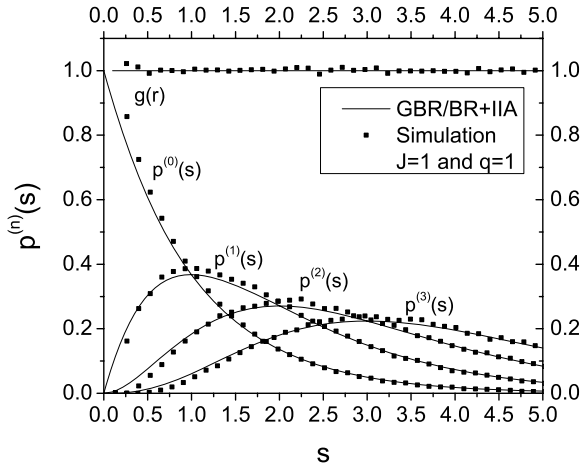

Figure 11. Spacing distribution function in the NESS for $J = 1$. We took data of three different times $t/L = 10, 100, 1000$ with $L = 200$.

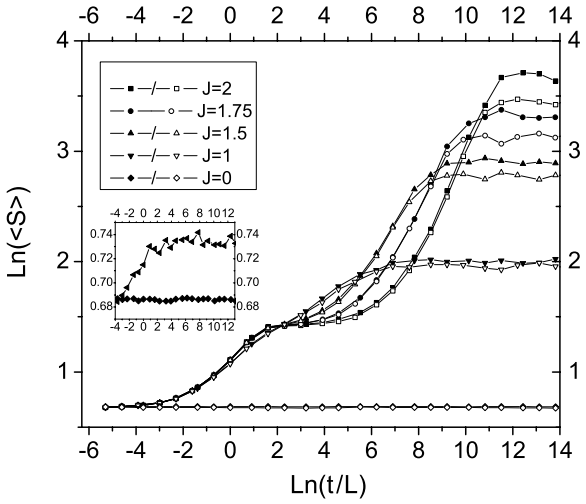

Figure 12. Average length for different values of J. Open symbols: $L = 100$ and filled symbols: $L = 200$. In the inset we compare $J = 0$ and $J = 0.1$ for $L = 200$ in order to verify the domain formation for small values of J.

of J (with $E = T = 1$). In fact for $J = 1$ this region is absent but for bigger values of J its size increases. Nevertheless, $\langle S(t)\rangle$ does not seem to depend on the length of the system in the scaling regime, it is the same for $L = 100, 200, 500$, the differences arise near to the NESS naturally[3]. In figure 12, for $J = 2$, the system seems to reach another metastable state where $\langle S(t)\rangle \approx 40$ for $N = 200$ and $\langle S(t)\rangle \approx 30$ for $N = 100$. For $J = 2$, the scaling region has a considerable duration but this duration is smaller for lower values of J. From figure 12, it is evident that the value of $\langle S(t)\rangle$ in the NESS regime depends on the size of the system, as

[3] The case $L = 500$ was verified but is not included in the figure.

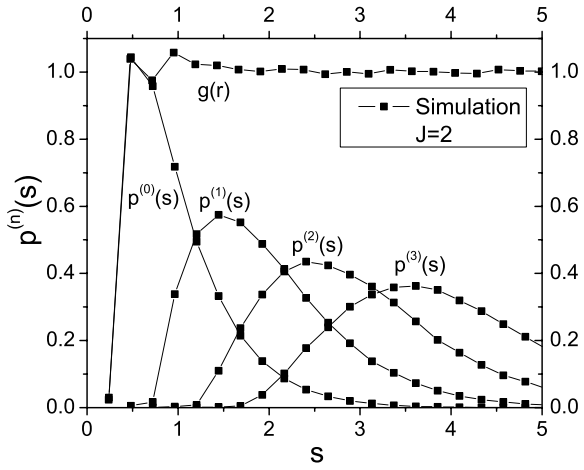

Figure 13. Statistical behavior of the metastable state in the spin system for $J = 2$. We took data at three different times: $T/L = 10, 20, 30$.

also happens in the gas system. In the inset of figure 12, we compare $\langle S(t)\rangle$ for $J = 0$ and $J = 0.1$, in the last case there is domain formation and it seems that only for $J = 0$ is there no domain formation.

As also happens in the gas system, the statistical behavior of this model is better described by the Berry–Robnik+IIA than the generalized Berry–Robnik model. In figure 14, we show the statistical behavior of the system for different values of J. For $J = 0$, the system evolves in time remaining disorganized, as we expected. However, we cannot compare directly its spacing distributions with our analytical model because of the effects of the discrete finite lattice that we use in our simulations. In fact, as we can see in figure 14, $p^{(0)}(1/2) = 1$ instead of $p^{(0)}(0) = 1$ as predicted by the continuous Poisson distribution. This result can be understood if we remember that, in a lattice, the lowest value for which the nearest spacing distribution is defined is $s = \rho(t)$, with $\rho(t)$ being the density of particles. In our case, $\rho(t) = 1/2$ for $J = 0$ in each spin species. This technical problem is usually solved taking low-density values as we did in the PCRW, where we took $\rho(0) = 1/10$. However, we cannot do this in the spin system. We have to take small lattices because the simulation is very intensive and low densities give us a poor statistic. This is only a technical problem and we can be sure that in the limit of low densities and small values of J, the system is well described by the continuous Poisson distribution. To corroborate this, we compare the results of our simulation for $J = 0$ with the discrete version of the Poisson distribution ($p^{(0)}(s) = (1/2)^{2s-1}$, $p^{(1)}(s) = (2s-1)(1/2)^{2s-1}$, etc).

For $J = 2$ the system sets into an organized state where there is domain formation. In this case, $p^{(0)}(s)$ is well fitted by the Wigner distribution. For $J = 2$, the results of our microscopic simulation coincide with the results of the macroscopic array domain simulation in the regime $T \ll E \ll J$. For intermediate values, the system shows a mixed state. If we do not take into account the discrete finite lattice, for all values of J, $p^{(n)}(s)$ is well described by the Berry–Robnik+IIA model. This suggests that for this system the correlations between domains are not strong as happens in the gas system. For low densities and values of J near 1, we expect that the generalized Berry–Robnik and the Berry–Robnik+IIA model are a good approximation for higher spacing distribution functions ($n > 1$) and for the

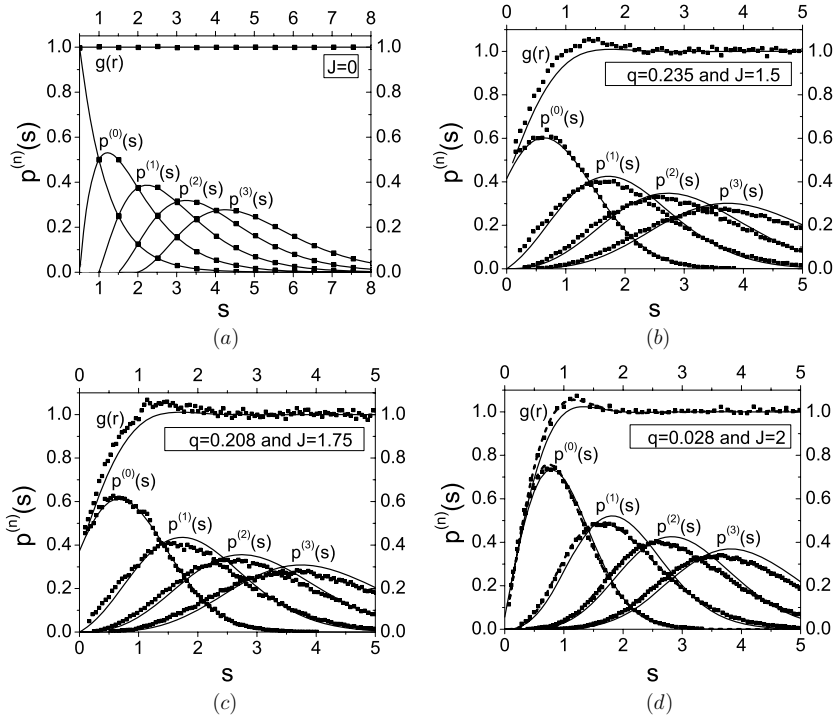

Figure 14. Crossover for the spin system.

pair correlation function because in this regime the correlation between domains can be neglected.

In our numerical simulations we took $\mu = 0.5$ and 2000 realizations. The measures were taken at different times using two lattices: $L = 500$ and $L = 200$, in order to confirm the scaling property. For $J = 2$, we took $t/L = 10000$ and $t/L = 4000$ for $L = 500$ and $L = 200$. For $J = 1.75$, we took $t/L = 9000$ for $L = 500$ and $t/L = 6000, 7500, 9000$ for $L = 200$. For $J = 1.5$, we took $t/L = 2000$ for $L = 500$ and $t/L = 1500, 2000$ for $L = 200$. For $J = 0$, the system remains disorganized and the time when the data are taken is irrelevant.

6. Conclusion

In all systems considered in this paper, the original Berry–Robnik model gives us a good fit for the nearest neighbor distribution $p^{(0)}(s)$, i.e., $p^{(0)}(s)$ can be approximated by the uncorrelated superposition of one Wigner and one Poisson distribution function. The biggest differences in the fits are given when the densities of both sequences have similar values. We calculate the next spacing distribution functions by using two methods: the GBR and the BR+IIA. We found that the GBR model gives us a good approximation for the statistical behavior of the PCRW and the BR+IIA model is a good approximation for the gas and spin systems. This fact suggests that the correlations between domains in the gas and spin systems are not strong and can be neglected in a first approximation but in the PCRW the correlations between particles cannot be neglected.

Our analytical models are simple and allow us to have a quantitative measure of the degree of order/disorder of the systems through the parameter q. For $q = 1$ the system is completely disordered and $p^{(0)}(s)$ is described by the Poisson distribution, this means that the system is homogeneous, in the statistical average sense. For $q = 0$ the system is organized and $p^{(0)}(s)$ is described by the Wigner distribution. In the particular case of the PCRW $q = 0$ implies that there is an effective repulsion between particles and in the case of the gas and spin systems it means domain formation. Unfortunately, the information about the interaction between particles/domains cannot be extracted easily from the statistical behavior in non-equilibrium systems. However, by using the BR+IIA model it is possible to calculate in an approximate way the interaction potential between domain borders for the gas and spin systems, as follows. Comparing (33) with a Boltzmann factor with an inverse temperature $\beta = 1$ it is straightforward to show that, under the BR+IIA approximation, the statistics of the domain borders is approximately equivalent to a system with N particles which interact according to the potential

$$V_N(x_1, \ldots, x_N) = \sum_{i=1}^{N} q(x_{i+1} - x_i) - \sum_{i=1}^{N} \ln[f(x_i, x_{i+1})], \tag{40}$$

where

$$f(x_i, x_{i+1}) = q^2 \operatorname{erfc}\left(\frac{\sqrt{\pi}}{2}(1-q)s\right) + \left(2q(1-q) + \frac{\pi}{2}(1-q)^3 s\right) \mathrm{e}^{-\frac{\pi}{4}(1-q)^2 s^2}, \tag{41}$$

and $s \equiv x_{i+1} - x_i$. Thus, the statistics of the domain edges of the gas and spin systems in their crossover regimes is approximately equivalent to a statistical equilibrium system of particles on a circle interacting through the nearest neighbor pair potential (40). Note that for $q = 0$, equation (40) reduces to

$$V_N(x_1, \ldots, x_N) = \sum_{i=1}^{N} \left[\frac{\pi}{4}\left(x_{i+1} - x_i\right)^2 - \ln\left(\frac{\pi}{2}\left(x_{i+1} - x_i\right)\right)\right], \tag{42}$$

as we can expect from [5]. Naturally, for $q = 1$ the interaction potential is a constant and the interaction force between domain edges vanishes.

In the crossover between order and disorder, all systems lose their level repulsion properties, i.e., the correlations between domains/particles decrease. In the PCRW, the correlations between particles arise from the coalescence reaction for $k > 0$, in the gas case, correlations arise from the mutual obstruction of particles for $\gamma < 1$. For the spin system, taking $E = 1$ and $T = 1$, the crossover depends only on J and the correlations arise for $J > 0$.

The gas and spin systems have a similar statistical behavior in the crossover between organized and disorganized states but $\langle S(t) \rangle$ is very different in the two cases. The metastable regions that we found in the spin system are not present in the gas system nor in the PCRW. In fact metastable regions are not predicted by the macroscopic dynamical rules used in [12]. In the PCRW, there is a time τ_1 when the interaction goes unnoticed which depends on the parameter k. In the gas and spin systems it seems that this time does not depend on the parameters γ and J respectively.

Finally, for the PCRW, we found that the parameter $q \equiv q(\tau, k)$, which characterizes the crossover, can be scaled in a function of a single argument $\tilde{\tau}$ by making the change of variable $\tilde{\tau} = \tau k^2/(1-k)^2$. The scaling factor is proportional to the crossover time between the intermediate regime and the long-time regime, τ_2.

Acknowledgments

The authors would like to thank F van Wijland for valuable comments and observations. This work was partially supported by an ECOS Nord/COLCIENCIAS action of French and Colombian cooperation and by Comité de Investigaciones y Posgrados, Facultad de Ciencias, Universidad de los Andes.

References

[1] Berry M V and Robnik M 1984 Semiclassical level spacings when regular and chaotic orbits coexist *J. Phys. A: Math. Gen.* **17** 2413–21
[2] Jacquod P and Amiet J P 1995 Evidence for the validity of the Berry–Robnik surmise in a periodically pulsed spin system *J. Phys. A: Math. Gen.* **28** 4799–811
[3] Lopac V, Brant S and Paar V 1996 Level density fluctuations and characterization of chaos in the realistic model spectra for odd–odd nuclei *Z. Phys.* A **356** 113–8
[4] ben-Avraham D and Havlin S 2000 *Diffusion and Reactions in Fractals and Disordered Systems* (Cambridge: Cambridge University Press)
[5] González D L and Téllez G 2007 Statistical behavior of domain systems *Phys. Rev.* E **76** 011126
[6] González D L and Téllez G 2007 Is the nearest neighbor distribution enough to describe the statistical behavior of a domain system? *Proc. Conf. Traffic and Granular Flow 2007* (at press)
[7] ben-Avraham D and Brunet É 2005 On the relation between one-species diffusion-limited coalescence and annihilation in one dimension *J. Phys. A: Math. Gen.* **38** 3247–52
[8] González D L and Téllez G 2008 Wigner domains for domain systems *J. Stat. Phys.* **132** 187–205
[9] Zhong D and Ben-Avraham D 1995 Diffusion-limited coalescence with finite reaction rates in one dimension *J. Phys. A: Math. Gen.* **28** 33–44
[10] Privman V and Doering C R 1993 Crossover from rate-equation to diffusion-controlled kinetics in two particle coagulation *Phys. Rev.* E **48** 846–51
[11] Mettetal J, Schmittmann B and Zia R 2002 Coarsening dynamics of a quasi one-dimensional driven lattice gas *Europhys. Lett.* **58** 653–9
[12] Cornell S J and Bray A J 1996 Domain growth in a one-dimensional driven diffusive system *Phys. Rev.* E **54** 1153–60
[13] Spirin V, Krapivsky P L and Redner S 1999 Coarsening in a driven Ising chain with conserved dynamics *Phys. Rev.* E **60** 2670–6
[14] Alemany P A and ben-Avraham D 1995 Inter-particle distribution functions for one-species diffusion-limited annihilation, $A + A \rightarrow 0$ *Phys. Lett.* A **206** 18–25
[15] Derrida B, Hakim V and Zeitak R 1996 Persistent spins in the linear diffusion approximation of phase ordering and zeros of stationary Gaussian processes *Phys. Rev. Lett.* **77** 2871–4
[16] Majumdar S N, Sire C, Bray A J and Cornell S J 1996 Nontrivial exponent for simple diffusion *Phys. Rev. Lett.* **77** 2867–70
[17] Krapivsky P L and Ben-Naim E 1997 Domain statistics in coarsening systems *Phys. Rev.* E **56** 3788–98
[18] Ben-Naim E and Krapivsky P L 1998 Domain number distribution in the non-equilibrium Ising model *J. Stat. Phys.* **93** 583–601
[19] Salsburg Z W, Zwanzig R W and Kirkwood J G 1953 Molecular distribution functions in a one-dimensional fluid *J. Chem. Phys.* **21** 1098–107